ISSN 1330-3651
UDC/UDK 620.172/.176:669.14-272

MODEL FOR FATIGUE LIFETIME PREDICTION OF TORSION BARS SUBJECTED TO PLASTIC PRESETTING

Vinko Močilnik, Nenad Gubeljak, Jožef Predan

Original scientific paper

The torsion presetting of a spring-bar is a common technique for extending the elastic twist-angle and increasing torque, but it reduces fatigue lifetime. Spring-bars are used as shock absorbers in caterpillar machines. Spring-bars, made from high strength fine-grain steel, grade VCN, provide a high level of absorbed energy. Any slight change in the presetting procedure has a strong influence on fatigue-lifetime. Within the same loading range, springs can exhibit low-cyclic or high-cyclic fatigue behavior regarding different presetting levels. A model for fatigue-lifetime and shear-stress levels is proposed on the basis of performed tests. Considering prescribed fatigue tests, it is possible to optimize a spring bar's geometry, in order to survive the required number of cycles.

Keywords: *presetting, torsion, spring-bars, fatigue, lifetime, cyclic fatigue, torque, spring steel*

Model za predviđanje zamornog vijeka trajanja torzijskih štapova podvrgnutih plastičnom prednaprezanju

Izvorni znanstveni članak

Prednaprezanje torzijskog štapa je uobičajena metoda za povećanje elastičnog kuta uvijanja i zakretnog momenta, ali ono skraćuje vijek trajanja do zamora. Opruge se koriste kao prigušivači kod strojeva s gusjenicama. Opruge, napravljene od sitno zrnatog čelika visoke čvrstoće, klase VCN, omogućuju visoki nivo absorbirane energije. Svaka i najmanja promjena tijekom postupka prednaprezanja ima veliki utjecaj na vijek trajanja do zamora. Unutar istog opterećenja, opruge mogu pokazati nisko ili visoko cikličko ponašanje na zamor u odnosu na različite stupnjeve prednaprezanja. Na osnovi izvršenih ispitivanja predlaže se model za vijek trajanja do zamora i nivoe smičnog naprezanja. Uzimajući u obzir provedena ispitivanja na zamor, moguće je optimizirati geometriju torzijskog štapa kako bi izdržao željeni broj ciklusa.

Ključne riječi: *prednaprezanje, uvijanje, torzijski štap, zamor, radni vijek, ciklički zamor, zakretni moment, čelik za opruge*

1 Introduction

The qualities of springs play a significant role in regard to their fatigue-lifetimes in the cases of low and high-cyclic fatigue. Round spring-bars are commonly used as springs for vehicles and caterpillar machines. A spring's quality depends on its material microstructure, and the thermo-mechanical treatment of the springs during the manufacturing process. The final cold-rolling defines the final shape and surface-roughness of a spring. The process of cold-rolling reduces any stress concentration caused by surface-roughness. It is well-known that it is possible to achieve a higher suspension angle by presetting the spring [1, 7]. Compressive residual stress caused by presetting appears at the outer boundary of the spring's body. It is accepted that the extension of a torsion spring's lifetime is achieved by cold-rolling its surface. Surface defect can cause additional stress concentration, and a reduction of lifetime. Properly performed presetting of the torsion bar-spring usually leads to a higher elastic twist-angle, in contrast to a spring bar without presetting [1, 6, 7]. In order to enlarge the angle of elasticity, the springs are torsion-deformed into a plastic during the manufacturing process. The preferred method is the elastic-plastic presetting of the bar. The bar is twisted within the plastic shear-zone over a specified angle, unloaded, and twisted at least twice to the same twist-angle. The measurement for plastic presetting is the angle size over the yield's shear-angle. Presetting causes plastic shear-strain at the outer boundary of the spring bar, meanwhile only the material in the middle of the bar remains elastically-deformed. It causes compressed residual stress at the outer boundary of the spring bar. This paper aims to analyse the effects of different presetting twist-angles on fatigue lifetime, under differently applied strains.

2 Material and specimens

Torsion-bar specimens were made from high-strength spring fine-grain steel, grade *VCN* [5]. The chemical composition is listed in Table 1 as a weight %. The used spring's material was rolled, forged, and soft- annealed during the manufacturing process. Specimens were made according to the same technological procedure as regular spring production. The final shape and spring properties were achieved by the following mechanical process: programmed turning, milling, and polishing of the spring's body to a roughness of $Ra \leq 0{,}2$ μm. The geometry of a specimen is shown in Fig. 2, diameter $d = 10$ mm and a torsion-relevant length of $l = 250$ mm. Fig. 1 shows the theoretical relationship between the shear-strain and twist-angles, by considering the diameter and length of the spring bar.

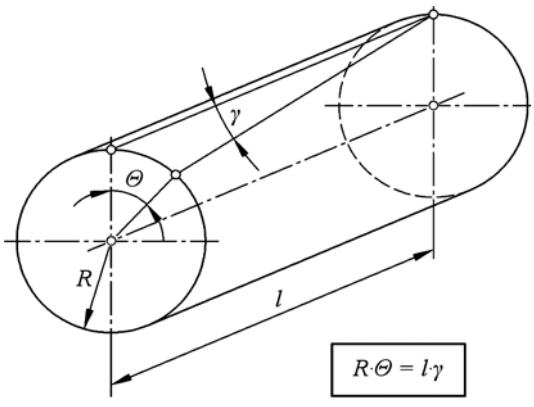

Figure 1 Twist angle Θ and shear strain γ at the torsion bar ($R = d/2 = 5$ mm)

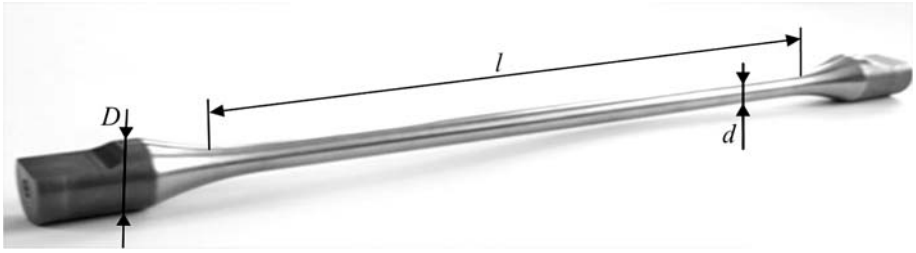

Figure 2 Specimen of torsion bar spring

Table 1 Chemical composition and mechanical properties of spring steel

	C	Si	Mn	Cr	Ni	Mo	V	Cu	P	S
%	0,44	0,28	0,56	0,87	1,41	0,26	0,11	0,12	0,009	0,002
UTS R_m / MPa	Yield $R_{p0,2}$ / MPa		Torsion limit τ_e / MPa		Shear modulus G / GPa		Modulus E / GPa		Hardness HRc	
2010	1570		800		75		193		52 - 55	

3 Torsion presetting of bar springs

Fig. 3 shows an experimentally-obtained shear stress-strain curve [2, 22]. As shown in Fig. 3, this is characterized by a shear stress-strain diagram for which the material undergoes an increasing amount of shear-strain when the shear-stress in the material reaches the yield point τ_e. Thus, as the applied torque increases in magnitude above the yield point, it will begin to cause plastic strain. Firstly at the outer boundary of the bar and then, as the maximum shear strain increases, to the yielding boundary and progressively inwards towards the bar's centre, (Fig. 4a). In regard to different preset-twist angles, the magnitude of stress is different, as shown in Fig. 4b) for angles of twist 37°, 45° and 57°, respectively. The result of presetting torsion bar springs within a plastic region is an extension of the elastic torsion angle by 25 %. Robustness is required for vehicles when off-road because impacted hits and shocks to tyres can appear, e.g. Land Rovers, Caterpillar vehicles. When the bar-spring is subjected to torsion above the yield- point, compressed residual stress appears at the outer boundary, it is thus in balance with the elastic torsion-stress in the middle of the cross-section.

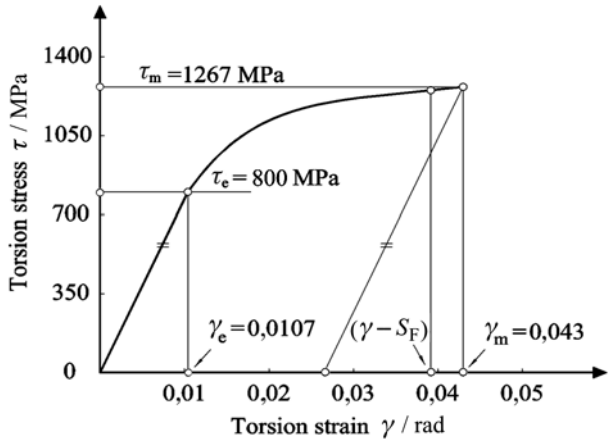

Figure 3 Reduction of γ_m, for S_F a safety factor

The maximum preset strain γ_m is limited by the ultimate shear strength τ_m of the material. For safety reasons, the maximum allowed preset strain should be lower than γ_m at a safety factor of S_F, usually 5 % of the corresponding torque regarding τ_m, as shown in Fig. 3. It is well-known that the shear-strain distribution over a radial line on a shaft is based on geometric consideration, and always remains linear. The shear-stress distribution, however, depends on the applied torque and must, therefore, be determined from the materials behaviour using a stress-strain diagram, Fig. 3.

Plastic torque reversal causes an elastic shear-strain through the bar. The new elastic shear limit is higher and it is possible to calculate stress-distribution over a spring's cross-section by the use of super positioning between residual stresses and applied stress-distribution [1, 7]. The compressed residual stresses at the outer boundary of the specimen contribute to a reduction in maximal shear-stress testing during torsion testing. Therefore, the shear-stress peak shifts from the outer boundary towards the bar's centre, as shown in Fig. 4a).

The force-produced stress is $dF = \tau \cdot dA = \tau \cdot r \cdot dr$. The stress distribution through the cross-section is given as a balance, using preset torque T_{ps}:

$$T_{ps} = \int_0^R r \cdot dF = 2 \cdot \pi \cdot \int_0^R \tau \cdot r^2 \cdot dr, \quad (1)$$

r is the polar radius where $r = 0$ in the centre of the bar's cross-section, and the maximum radius $R = d/2$ is at the outer boundary. τ is the shear-stress magnitude depending on the position on the cross-section. Distribution of the shear-stress $\tau(r)$ within the elastic loading regime is proportional to the torque:

$$\tau(r) = \frac{4 \cdot T_Y \cdot r}{\pi \cdot R^4}, \quad (2)$$

where T_Y is the torque at shear-yielding. In the case of elastic-plastic loading, shear-stress distribution $\tau(r)$ depends on the twist-angle Θ, and the torque $T(\Theta)$:

$$\tau(r, \Theta) = \frac{r}{\pi \cdot R^4} \cdot \left(\Theta \cdot \frac{dT}{d\Theta} + 3 \cdot T \right), \quad (3)$$

where T is the current torque, and twist-angle Θ is given in radians. Shear-stress distribution during a presetting process and consequently residual stress-distribution, is shown in Fig. 4 for preset angle Θ_{ps}=103°. Fig. 4a shows the

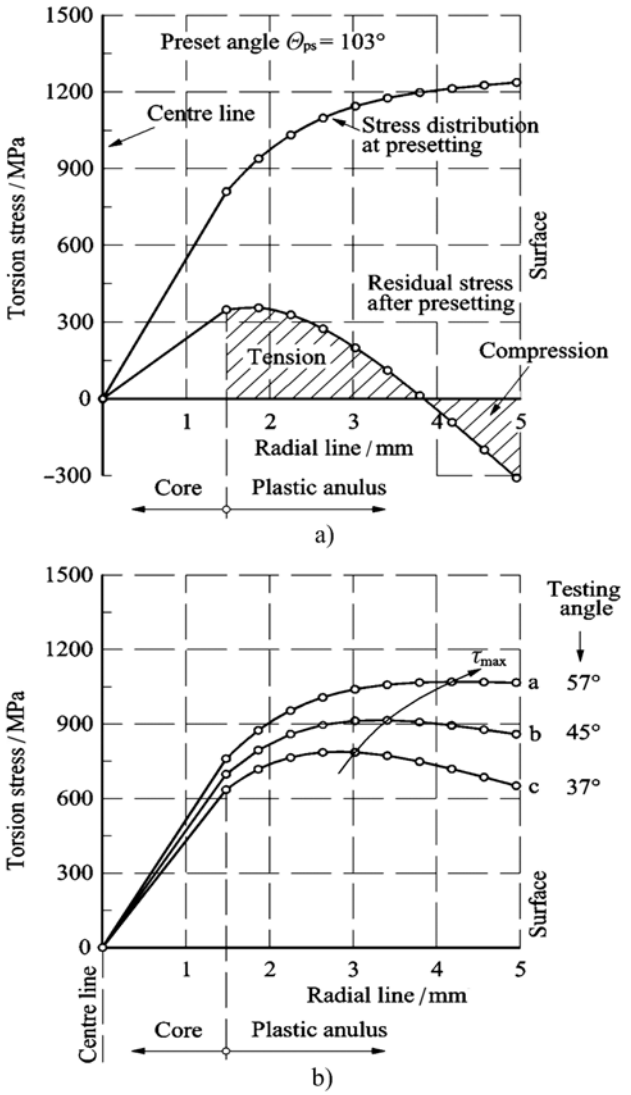

Figure 4 Shear stress distribution over a radial line of the spring bar obtained by analytical calculation [1, 7]: a) Stress distribution at presetting, and residual stress distributions after presetting; b) Final stress distribution obtained by super positioning of the tested and residual stress at three different twist angles

torsion-stress distribution during the presetting procedure. The residual stress-curve shows stress distribution after the presetting procedure, with a maximum compressed residual stress of –300 MPa at the outer boundary of the spring. The three curves, Fig. 4b show the results of super-positioning when testing linear-distributed torsion stress, in regard to the testing twist-angles Θ_t=57°, 45° and 37°, respectively.

4 Experimental results

4.1 Fatigue testing of torsion bars

Preset torsion-bars were tested on a mechanical testing device, as shown in Figs. 5a and 5b. The twist-angle Θ was adjusted by an eccentric crank on the testing device. The torque was measured by a commercial torque-cell (produced by HBM) with the following characteristics: nominal torque T_{nom}= 500 Nm, limit torque 150 % T_{nom}, ultimate torque >300 % T_{nom}, accuracy class 0,2 %, bridge supply 10 V and bridge-resistance 350 Ω. Data acquisition and analysis was done using Catman HBM software. The same testing machine was also used for elastic-plastic presetting, and fatigue testing.

Fatigue-tests were performed under a constant twist-angle Θ_t and loading ratio $R=T_{min}/T_{max}$= 0. A fatigue testing matrix was established for four differently preset twist-angles within preset twist-angle Θ_{ps} (37°, 47°, 67°, and 103°), and four fatigue twist-angles Θ_t (30°, 37°, 45°, and 53°). The selected preset twist-angles Θ_{ps} corresponded to the presetting-strain γ_{ps} during the manufacturing of torsion spring-bars for military vehicles [7]. The fatigue test twist-angles Θ_t (at the testing machine) are defined as corresponding values of applied shear-strain γ_t for vehicles. Different amounts of residual stress in the outer bounds of specimens should be obtained for differently preset elastic-plastic twist-angles. In order to avoid additional plastic shear strain, the angle of twist during fatigue-testing should be lower than the presetting angle ($\Theta_t < \Theta_{ps}$), by 5° at least. The testing matrix in Tab. 2 was created by considering the above-mentioned approach. The specimens in the upper-left area of Tab. 2 were not tested because their torsion loadings were higher than the new elastic angles after presetting the specimens. The no-presetting specimens can be subjected to twist-angle below γ_e. Note that the twist-angle is only =30,59° (or 0,534 rad) at shear-strain γ_e= 0,01068 rad.

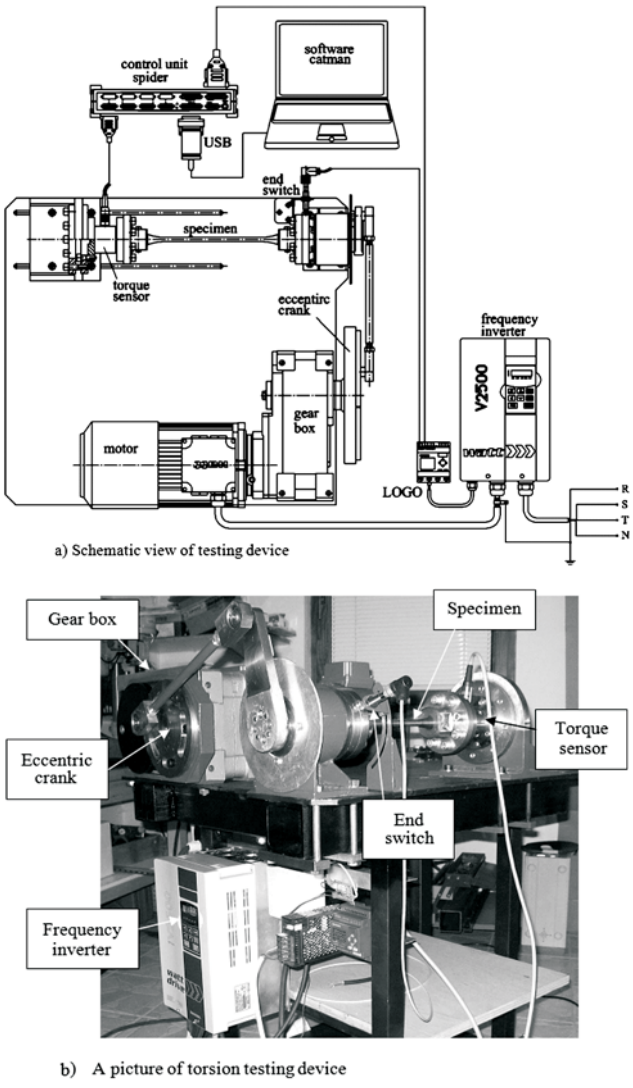

Figure 5 Device for the torsion testing of specimens: a) Schematic view and b) Photo of fixed specimen on eccentric crank machine

Table 2 Fatigue testing results for torsion bar springs subjected to a constant twist angle Θ_t

Presetting / Testing	Θ_{ps}=37° (γ_{ps}=0,0129) Θ_e=35°	Θ_{ps}=47° (γ_{ps}=0,0164) Θ_e=42°	Θ_{ps}=67° (γ_{ps}=0,0233) Θ_e=50°	Θ_{ps}=103° (γ_{ps}=0,0359) Θ_e=58°	Note-with increasing preset angle
Θ_t=53° (γ_t=0,0185)				(114 920)	
				66 777	
				80 768	
Θ_t=45° (γ_t=0,0157)			(1 141 198)	(774 662)	Decreasing ↓
			949 992	415 066	
			1 697 849	691 155	
Θ_t=37° (γ_t=0,0129)		3 139 315	4 592 192	5 053 741*	Increasing ↑
		2 985 906	4 509 632	5 004 937*	
		4 135 413			
Θ_t=30° (γ_t=0,0104)	*5 036 847	9 524 990	*5 121 997		

The tests' stopping criteria were either a torque's amplitude dropping by more than 10 %, or specimen failure, or a specimen-survival of more than five million cycles, whichever occurred first. The results are listed in Tab. 2. In those cases where the torsion-loading was much lower than the new elastic-angle, the specimens easily survived more than five million cycles, e.g. specimen preset at twist angle Θ_{ps}= 47°, and fatigued at a twist-angle of Θ_t= 30° failed after 9 524 990 cycles. Tests for specimens without failure or testing-torque are dropped by more than 10 % are marked by asterisks in Tab. 2. The presettings required for the tested-torques must always be in the direction of the preset-torque, and should never be reversed.

Tab. 2 shows the test results, the number of fatigue cycles until fracture, depending on the presetting and testing angle.

Θ_{ps} – Preset angle, °

Θ_t – Testing amplitude angle, °

Θ_e – New elastic angle after presetting, °

*– Testing sample with no fracture,

( ) – Testing sample with spiral fracture.

Tab. 2 shows that during testing at a twist-angle Θ_t = 45°, the number of cycles until failure significantly **decreases** as the preset twist angle Θ_{ps} **is increased** from 67° to 103°. In the same Tab. 2, it can be recognized that the testing twist-angle Θ_t = 37°, and the number of cycles until failure, significantly **increases** as the preset twist-angle Θ_{ps} **is increased** from 67° to 103°. Therefore, it can be concluded that a longer fatigue lifetime is obtained when the difference between the preset twist-angle Θ_{ps} and the maximum fatigue twist-angle Θ_t is higher. On the basis of these experimentally-obtained results, it is possible to plot a preset twist-angle-lifetime diagram as shown in Fig. 6.

Fig. 6 shows the range of fatigue testing results from the minimum to the maximum number of cycles. The ordinate shows the preset angle Θ_{ps}, and the abscissa the number of cycles where the specimens failed, or the torque-drop was

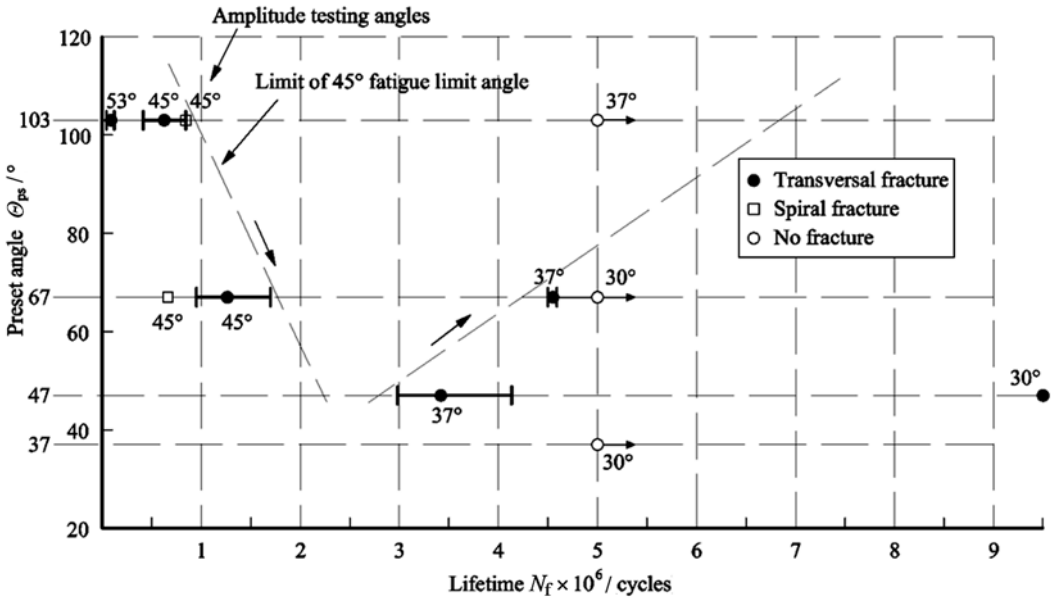

Figure 6 Average fatigue lifetime of round spring-bars under torsion vs. preset and tested amplitude angles

more than 10 %, or the specimens survived more than 5 000 000 cycles without a failure (marked as **no fracture**). The tested torsion-amplitude angle at any single point on the diagram is seen in Fig. 6. It can be seen that the average lifetime of a torsion bar-spring at lower torsion-loading increases at the same preset angle. The square symbol indicates those specimens with spiral fractures. In Tab. 2, these are shown inside the brackets, whilst the arrows in Fig. 6 indicate the specimens with no fractures. The duration of the testing process was very long, because the large testing-amplitude angle, and consequently, a lower number of specimens were tested.

4.2 Proposed model for fatigue lifetime

Despite a relatively small number of tested specimens, a model is proposed for fatigue-lifetime predictions regard preset twist-angle Θ_{ps} and fatigue- twist angle Θ_t. In order to ensure a more general approach, both twist-angles were defined in terms of preset shear-strain γ_{ps} and fatigue applied shear-strain γ_t. However, the proposed model is based on experimentally obtained results (see Tab. 2) and the used material (see Tab. 1) hence the approach used is more important than the obtained values of the model's parameters.

Fig. 7 shows the average number of cycles until the failure of the specimen. It is obvious that specimens subjected to lower torsion-stress amplitude achieve a higher number of cycles until fracture. It is possible to achieve a higher amplitude of testing torsion-stress if the applied shear strain is higher. Since the applied shear-strain γ_t is limited by the preset shear-strain γ_{ps}, the range of applied loading angle can be distinguished in a diagram, as shown in Fig. 7. Actually, the obtained results are given as a Wöhler's curve, as fatigue lifetime for the specified preset strain vs. maximum testing of shear-stress. Each line corresponds to one preset shear-strain γ_{ps} = 0,0164, γ_{ps}= 0,0233 and γ_{ps} = 0,0359, respectively. Since Wöhler's diagram is in logarithmic form (Fig. 7), shear stress can be approximated according to the power-law equation:

$$\tau_t = A_0 \cdot N_f^m, \tag{4}$$

where:
A_0 – Coefficient of the power law equation,
m – Exponent of the power law equation,
τ_t – Amplitude testing torsion stress, MPa,
N_f – Average lifetime until fracture.

Approximated values for the amplitude-testing of torsion-stress τ_t vs. number of cycles to failure N_f, are shown in the legend of Fig. 7, and listed in Tab. 3. It is obvious that each preset shear-strain γ_{ps} gives different values.

Coefficient A_0 and exponent m of the power-law equation from Fig. 7 are listed in Tab. 3 as a function of preset strain, and are shown in Figs. 8 and 9.

The values in Table 3 are plotted and interpolated by the power-law in Fig. 8. Functional dependence between coefficient A_0 and preset-strain γ_{ps}, can be given by an interpolation function between these three points. Note that this is only a proposed model. For a more accurate model and prediction it would be necessary to perform more tests with different preset elastic-plastic strains. However, it

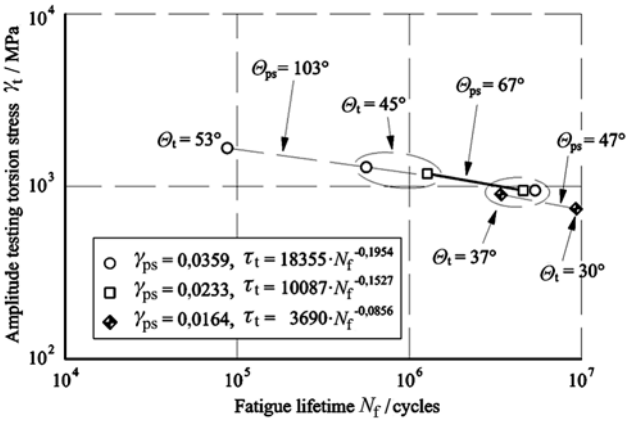

Figure 7 Fatigue lifetime vs. testing maximum torsion stress at different preset strains

Table 3 Values of coefficient A_0 and exponent m

Preset angle Θ_{ps}	γ_{ps}	A_0	m
103°	0,0359	3690	-0,0856
67°	0,0233	10087	-0,1527
47°	0,0164	18355	-0,1954

seems that exponent approximation is possible. Exponent m is also possible for expressing as a function of preset shear-strain γ_{ps}, for the obtained three points. Since all points lie on the same line, it is reasonable to use only linear interpolation for m vs. preset elastic-plastic strain γ_{ps}.

Both interpolations are limited by elastic-strain γ_{ps} = 0,01046 (on the left-side) and experimentally-obtained maximum shear-strain γ_{ps} = 0,043 (on the right-side). Therefore, both values (A_0 and m) are dimensionless and prescribed only within the plastic shear-strain range.

In the diagrams (Figs. 8 and 9) the coefficient A_0 and exponent m are approximated with the analytical functions marked in the diagrams. If for Eq. (4), you find a logarithm, and consider A_0 and m as a function of γ_{ps}, the number of cycles to failure can be expressed as a function of preset shear-strain γ_{ps} and an amplitude of torsion-stress τ_t, as follows:

$$\ln \tau_t = \ln A_0(\gamma_{ps}) + m(\gamma_{ps}) \cdot \ln N_f, \tag{5}$$

and

$$\ln N_f = \frac{\ln A_0(\gamma_{ps}) - \ln \tau_t}{-\left|m(\gamma_{ps})\right|}. \tag{6}$$

$$A_0(\gamma_{ps}) = 69\,686 \cdot e^{-82{,}019 \cdot \gamma_{ps}}. \tag{7}$$

$$m(\gamma_{ps}) = 5{,}5971 \cdot \gamma_{ps} - 0{,}2857. \tag{8}$$

It is possible to predict the lifetime N_f of a torsion bar spring by using the proposed model, as expressed in equations (4), (6), (7) and (8), as a function of the applied amplitude shear stress τ_t, (load ratio R = 0) , and the preset shear-strain γ_{ps}.

It is possible to express shear-stress τ_t, by using amplitude or the testing shear-strain γ_t as elastic, according to the Hooke's law

$$\gamma_t = \frac{\tau_t}{G}. \tag{9}$$

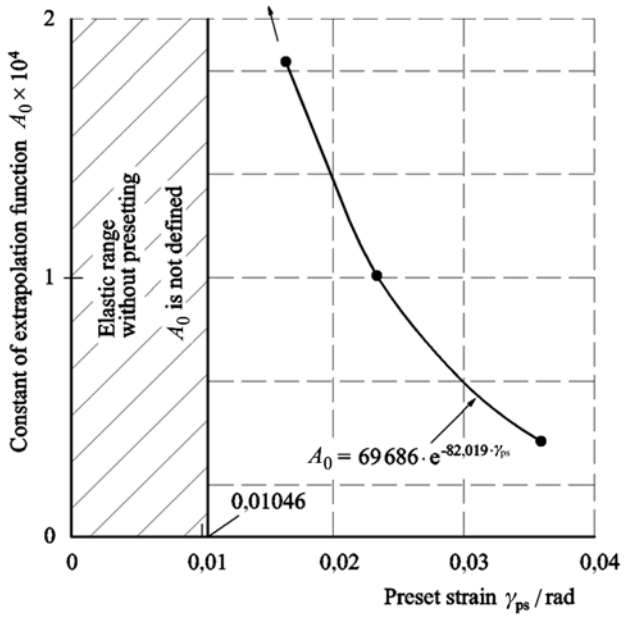

Figure 8 Coefficient A_0 of power law equation as a function of the preset strain

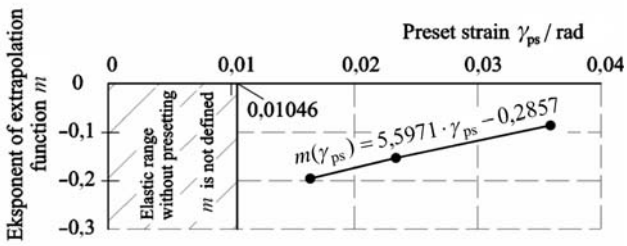

Figure 9 Exponent m of power law equation as a function of the preset strain

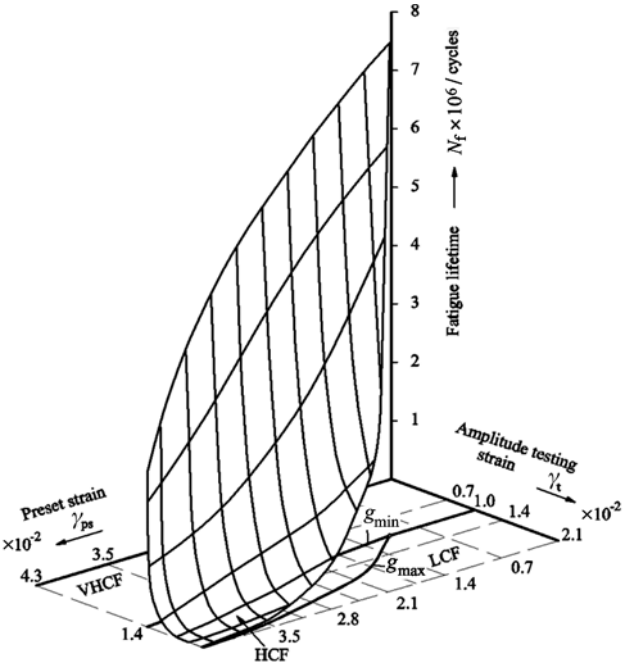

Figure 10 Fatigue lifetime of a torsion bar spring depending on the preset strain and amplitude testing strain, obtained on the basis of the model

Varying of the preset-strain and the amplitude of the testing-strain vs. the number of cycles to failure can be shown as a 3-D diagram, see Fig. 10. The average values for the number of cycles before failure lie on the space- surface of the 3-D diagram. The 3-D diagram of Fig. 10, has been created on the basis of bar-spring specimen testing until γ_{ps}=0,043, and on the basis of calculations by the model. Fig. 11 shows a ground-plan projection of the preset torsion-bar spring's usage area and testing stress, respectively (HCF - High Cyclic Fatigue). The hatched area in Fig. 11 represents the ground-plane projection of the 3-D surface of Fig. 10, limited by curves g_{max} and g_{min}. The so-called area of cyclical strength is limited by curves g_{min} and g_{max}. Under line g_{min} there is a range of very high-cyclical-fatigue (VHCF), where specimens have survived more than five million loading cycles. A range of low cyclical-fatigue (LCF) can be found over the curve g_{max}, because the cyclical plastic-strain should be taken into account. In fact the curve g_{max} presents the elastic limit-curve of the preset torsion bar-spring. Above g_{max} is a plastic strain-boundary.

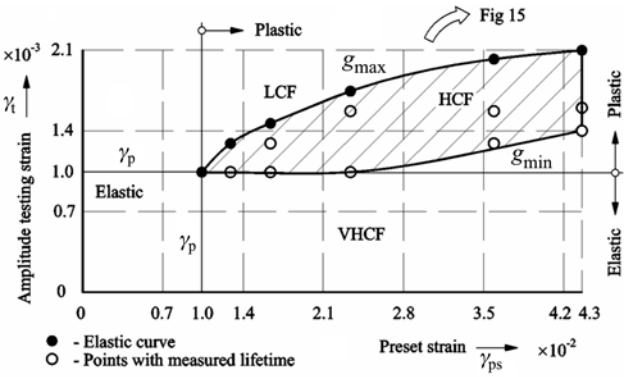

Figure 11 The regions of low, high and very high cyclic fatigue

The preset shear-strain and tested shear-strain of the torsion-bar spring should be inside the indicated area in Fig. 11. The indicated area over the preset-strain γ_{ps}= 0,0359 is used very rarely in practice, because the spring-bar survives over very few fatigue cycles. The tested loading range γ_t= 0,014 below the preset yield-point, actually has no effect on a lifetime of under five million loading cycles; it is a very high cyclical-fatigue area-VHCF. It should be noted, that the practical use of torsion-spring bars is for torsion-loadings of more than γ_t= 0,014, regarding the indicated area in Fig. 11. In this case, it is necessary to establish a model for predicting the fatigue-lifetime of torsion spring-bars. Customers (vehicle producers) require a minimum lifetime of around 10^5 loading cycles for a prescribed torsion-loading. Since the obtained results cover a range of $6{,}6\times10^4$ to 5×10^6 loading cycles, it is possible to apply the obtained results for a proposed model when predicting fatigue-lifetime is necessary. The calculated average number of cycles N_{fcal} is listed in Tab. 4 for each preset and applied strain. The differences between the predicted number of cycles and the experimentally- obtained numbers to failure N_{ftest} is within the range of ±11,3 %.

It corresponds to the usual scatter of experimentally-obtained results. Note that N_{ftest} is an average of the experimental results. However, it is possible to improve the model by performing more fatigue tests and statistical analyses of the results. A star in the field means that a fracture of the bar spring did not occur.

5
An optimization for the spring-bar's design

A torsion spring-bar (Fig. 12 - photo) is used for the suspension of impact and shocks during the driving of vehicles off-road. The spring-bar is fixed by a notched- end

Table 4 Calculated lifetime of bar springs in comparison with the measured ones

Θ_{ps} / °	γ_{ps} / rad	A_0	m	Θ_t / °	γ_t / rad	τ / MPa	N_{fcal}	$\overline{N}_{ftest}$	Err / %
47	0,0164	18159	-0,194	**30**	0,0104	781,9	10 702 237	9 524 990	**11,2**
47	0,0164	18159	-0,194	**37**	0,0129	969,8	3 629 225	3 420 211	5,7
67	0,0234	10246	-0,155	**37**	0,0129	969,8	4 066 002	4 525 912	**-11,3**
67	0,0234	10246	-0,155	**45**	0,0157	1180,3	1 148 876	1 263 013	-9,9
103	0,0359	3667	-0,085	**37**	0,0129	969,8	6 484 699	5 029 330	*
103	0,0359	3667	-0,085	**45**	0,0157	1180,4	644 139	626 961	2,6
103	0,0359	3667	-0,085	**53**	0,0185	1390,9	93 457	87 488	6,3

$\overline{N}_{ftest}$ - The average experimental measured number of cycles from Tab. 2
A star in the field means that the fracture of the bar spring did not occur.

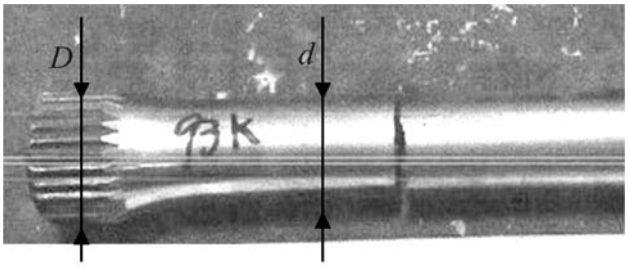

Figure 12 Photo of broken torsion spring-bar

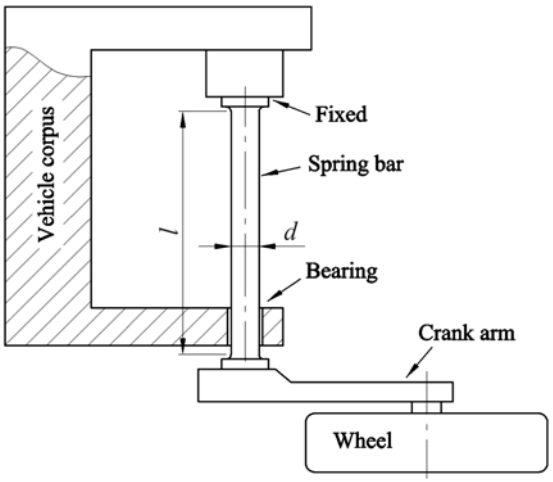

Figure 13 Suspension system of vehicle with a torsion spring-bar

in the vehicle's corpus on one side, and a guide-by bearing on the other side (as free rotation), as shown in Fig. 13. The crank arm of the wheel is at the radial free- end of the spring-bar. The twist-angle of the spring-bar is limited by the angle of the crank-arm as shown in Fig. 14. Usually, the boundary conditions are considering by using the:

- geometrical maximum diameter at the end D and torsion active diameter d,
- maximum length l of the spring-bar,
- loading as a minimum amplitude of torque T and minimum applied twist-angle (in terms of testing strain γ_t),
- optimum spring constant c,
- minimum fatigue lifetime over the number of cycles N_f.

Note that the ratio between the diameter at the end of spring D and the diameter of bar d should be high enough, in order to reduce stress concentration within the area of the radius!

Other parameters for spring-design and optimization at preset strain γ_{ps}, are given in Tab. 5, such as the material properties of the material (shear modulus G), spring-constant c, and the spring-mass. Fig. 15 shows a plastic part

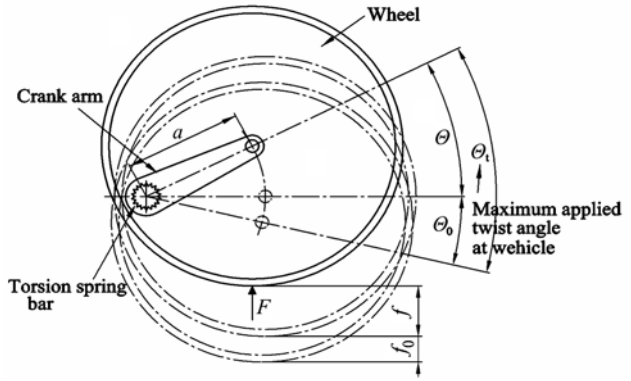

Figure 14 Crank arm of wheel with limited twist angle

from Fig. 11, limited by curves g_{max} and g_{min}. Fig. 15 shows the relationship between the testing-strain γ_t and preset-strain γ_{ps}, which is almost linear for a constant number of fatigue cycles N_f, by using the proposed model in Eq. (4), where A_0 and m are the coefficients given by Eqs. (7) and (8)!

Let us calculate three curves for the assumed constant lifetimes $N_f=10^5$, 3×10^5, and 6×10^5 fatigue loading cycles, by considering the preset strains γ_{ps}=2 %, 3 %, and 3,8 % . We only consider the lines inside the High Cycles Fatigue-HCF region, between g_{max} and g_{min}.

Since the minimum applied strain γ_t = 1,7 % is prescribed, we are looking for an area above this horizontal line.

Theoretically, any intersection points between the upper-limit and constant numbers of cycles, can be used, within the hatched area in Fig. 15, as appropriate value but, due to uncertainty, it is better to shift below the upper-limit curve g_{max} e.g. to points C and D. Therefore, any points in the optimum zone meet the given requirements. In regard to any reduction in stress concentration at the end of the spring, it is better to reduce diameter d of the round-section at the active part of the spring (point D), than looking for a higher number of cycles (point C). The spring-bar's diameter in point D is smaller, but since the spring-constant c must remain the same, the spring-bar's length can be reduced. Consequently, it is desirable to reduce the weight of the spring-bar. However, if the customer does not require any geometrical change and primarily needs the longest fatigue lifetime possible, in this case point C is optimum!

In a case where the amplitude of testing strain γ_t=1,7 % is fixed (also the twist-angle) thus increasing the preset strain e.g. γ_{ps} = 3,3 % (in point A) and γ_{ps} = 3,9 % (in point B) causes a decreasing of fatigue-lifetime.

As discussed, the established model provides the possibility for optimizing spring-design in terms of the size

Table 5 Optimization of a torsion spring bar (Figure 15)

		Requirement	Point A	Point B	Optimum lifetime Point C [2]	Optimum dimension Point D [1]
Preset strain	γ_{ps} / %	3.3	3.3	3.9	2.37	3.3
Testing strain	γ_t / %	min 1.7	1.7	1.7	1.7	1.93
Shear modulus	G / MPa	75183	75183	75183	75183	75183
Testing stress	τ_t / MPa	min 1251.4	1278.1	1278.1	278.1	1454
Fatigue lifetime	N_f / cycles	min 100 000	300 000	100 000	600 000	100 000
Amplitude torque	T / N·m	min 52280	52280	52280	52280	52280
Spring diameter	d / mm	max 59.7	59.2	59.2	59.2	56.7
Spring length	l / mm	max 2004	1947.2	1947.2	1947.2	1639.6
Spring constant	c / N·m/°	817.2	817.2	817.2	817.2	817.2
Spring mass	m' / kg	max 44.0	42.1	42.1	42.1	32.5
Model values						
A_0	-	-	4652.35	2844.13	9975.67	4652.35
m	-	-	-0.101	-0.067	-0.153	-0.101

[1] An optimum regarding torsion-loading with reduced mass
[2] An optimum regarding fatigue-lifetime

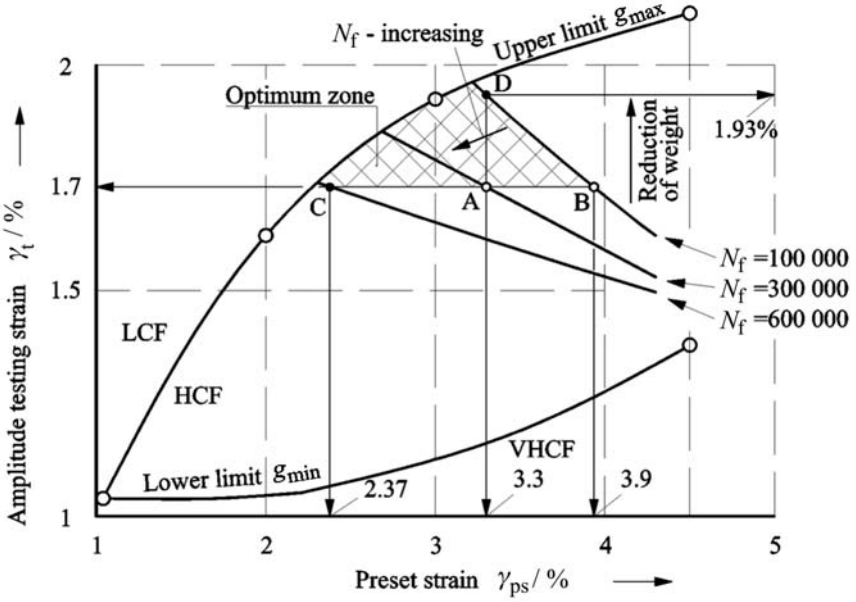

Figure 15 Determination of optimum zone in respect to requirements and experimentally obtained fatigue behavior after elastic-plastic presetting

(e.g. weight) of the spring and/or the fatigue-lifetime of the spring.

6 Conclusions

A spring made as a torsion-bar exhibits different fatigue behavior in regard to different elastic-plastic preset torques. The aim of this paper was an analysis of different effect, when presetting a twist-angle regarding fatigue lifetime under differently applied strains. Presetting causes plastic shear-strain at the outer boundary of the spring-bar, meanwhile the material in the middle of bar remains elastically-deformed. Since the outer part remains plastically-deformed, the spring bar cannot restore itself to the start position, and the inner- part of the section remains elastically loaded. It causes compressed residual stress at the outer boundary of the spring-bar. It is possible to increase the twist angle by increasing the elastic-plastic presetting of the torsion-bar, but this causes a reduction in fatigue lifetime. The experimentally obtained results show that fatigue-lifetime strongly depends on the ratio between **the loading at presetting** and **the fatigue-loading range**. In spite of a relatively small number of tested specimens, a model has been proposed for fatigue lifetime and shear-stress level. The established model provides the possibility for optimizing a spring-design in terms of the size (e.g. weight) of the spring. Optimum zone boundaries are determined by the fatigue-behavior of the tested specimens, the material properties, and the customer's requirements.

Since the optimum zone is within a range of acceptable solutions, the main target of optimization can be:

a) a reduction in stress concentration at the end of the spring by reducing the diameter and twist-length of the spring, which leads to a reduction in the spring-bar's weight, or
b) the highest number of fatigue cycles under the required twist-angle, proportional to the fatigue shear-strain.

7 Used symbols

A_0 – Coefficient of the power law equation, –
d – Spring diameter, mm
E – Modulus of elasticity, MPa
G – Shear modulus, MPa
g_{min} – Lower limit functions, –
g_{max} – Upper limit function, –
l – Spring length, mm
m – Exponent of power law equation, –
T – Amplitude torque, N·m
T_{ps} – Preset torque, N·m
$T_Y = T_e$ – Elastic limit torque, N·m
T_{min} – Minimum torque, N·m
T_{max} – Maximum torque, N·m
T_m – Ultimate torque, N·m
N_f – Lifetime until fracture, cycles
R – Spring radius, mm; Loading ratio, –
Ra – Surface roughness, μm
$R_{p0,2}$ – Yield strength (σ_Y), MPa
R_m – Ultimate tensile strength (UTS), MPa
S_F – Safety factor, –
τ – Torsion stress, MPa
τ_e – Torsion elastic limit (τ_Y), MPa
τ_t – Testing amplitude torsion stress, MPa
τ_m – Torsion strength, MPa
γ – Torsion strain, rad, %
γ_t – Torsion testing amplitude strain, rad, %
γ_{ps} – Preset strain, rad, %
γ_m – Strain at torsion strength, rad, %
Θ – Twist angle, °
Θ_t – Testing amplitude angle, °
Θ_{ps} – Preset angle, °
Θ_e – New elastic angle after presetting, °.

8 Abbreviations

HCF – High cyclical fatigue
HRc – Rockwell hardness
LCF – Low cyclical fatigue
UTS – Ultimate tensile strength
VHCF – Very high cyclical fatigue.

9 References

[1] Hibbeler, R. C. Mechanics of Materials-sixth edition. Pearson Prentice Hall, New Jersey, USA, 2005.
[2] Močilnik, V.; Vpliv prednapetja na dinamično nosilnost vzvojne vzmeti. Doktorska disertacija. Fakulteta za strojništvo Maribor, 2009.
[3] Farahmand, B. Fatigue and Fracture Mechanics of High Risk Parts. Chapman & Hall, Dept. BC, New York, 1997.
[4] Kalluri, S.; Bonacuse, P. Multiaxial Fatigue and Deformation: Testing and Prediction. ASTM STP 1387, West Conshohocken, 2000.
[5] Dobi, Đ. Ciklične karakteristike jekla TORKA. // Železarna Ravne na Koroškem-SLO, ustvarjalna naloga, (1987).
[6] SAE, Manual on Design and Manufacture of Torsion Bar Springs And Stabilizer Bars. // Society of Automotive Engineers, HS-796(2000).
[7] Milinković, B. Pomeranje granice elastičnosti torzionih štapova primenom prethodnog naprezanja. // Naučno-tehnički pregled Beograd. 6(1984), 16-25.
[8] Močilnik, V.; Gubeljak, N.; Predan, J.; Flašker, J. The Influence of Constant Axial Compression Pre-stress on the Fatigue of Torsion Loaded Tube Springs. // Enginering Fracture Mechanics, 77, 16(2010), 3132-3142.
[9] Thompson, K. D.; Sheppard, S. D. Stress intensity factor in shafts subjected to torsion and axial loading. // Engineering Fracture Mechanics, 42(1992), 1019-1034.
[10] Marquis, G.; Socie, D. Long Life torsion fatigue with normal mean stresses. // Fatigue Fract. Engng. Mater. Struct. 23(2000), 293-300.
[11] Rozumek, D.; Marciniak, Z.; Lachowicz, T. C. The energy approach in the calculation of fatigue lives under non-proportional bending with torsion. // International Journal of Fatigue, 32(2010), 1343-1350.
[12] Makabe, C.; Socie, D. F. Crack growth mechanisms in pre-cracked torsion fatigue specimens. // Fatigue Fract. Engng. Mater. Struct. 24(2001), 607-615.
[13] Zang, W.; Akid, R. Mechanism and fatigue performance of two steels in cyclic torsion with axial static tension/ compression. // Fatigue Fract. Engng. Mater. Struct., 20(1997), 547-557.
[14] McClaflin, D.; Fatemi, A. Torsional deformation and fatigue of hardened steel including mean stress and stress gradient effects. // International Journal of Fatigue, 26(2004), 773-784.
[15] Tabernig, B.; Pippan, R. Effect of periodic overloads in particle- reinforced aluminium alloys: the near threshold behaviour. // International Journal of Fatigue 26(2004), 323-330.
[16] Pippan, R.; Bichler, C.; Tabernig, B.; Weinhandl, H. Overloads in ductile and brittle materials. // Fatigue Fract. Engng. Mater. Struct. 28(2005), 971-981.
[17] Flaceliere, L.; Morel, F.; Dragon, A. Coupling between Mesoplasticity and Damage in High-cycle Fatigue. // International Journal of Damage Mechanics, 16(2007), 473-509.
[18] Couroneau, N.; Royer, J. Simplified model for the fatigue growth analysis of surface crack in round bars under mode I. // International Journal of Fatigue, 10(1998), 711-718.
[19] Aernoudt, E.; Snoeys, R. Der Torsionsversuch, ein Verfahren zur Messung der plastischen Eigenschaften von Metallen. // Drahtwelt, 59(1973), 170-177.
[20] Kloos, K. H.; Koch, M.; Kaiser, B. Eigenspannungs-messungen an unterschiedlich abgekohlten, kugelgestrahlten und torsionsschwellbeanspruchten Proben aus Federstahl. // *Z.* Werkstofftech, 17(1986), 350-356.
[21] Chapetti D. M. Prediction of threshold for very high cycle fatigue ($N>10^7$ cycles). // Proceeding Engineering, 2(2010), 257-264.
[22] Gubeljak, N.; Močilnik, V.; Predan, J. Fatigue Failure of Pre-stressed Torsion Bar. // 4th International Conference "Fracture Mechanics of Materials and Structural Integrity", Ukrajina L'viv, 22. do 27. jun 2009. L'viv: Fiziko-mehanični institut im. G.V., Karpenka NAN Ukraina 2009, 203 – 209.
[23] Shariati, M.; Sedighi, M. Saemi, J.; Reza Allahbakhsh, H. A numerical and experimental study on buckling of cylindrical panels subjected to compressive axial load. // Strojniški vestnik - Journal of Mechanical Engineering, 56, 10 (2010), 609-618.

Authors' addresses

Dr. Vinko Močilnik
ERD d.o.o., Engineering, Design & Development
Črneče 186, 2370 Dravograd, Slovenia
Tel.: +386-31-331-664
E-mail: vinko.mocilnik@siol.net

Prof. dr. Nenad Gubeljak
University of Maribor
Faculty of Mechanical Engineering
Smetanova ul. 17, 2000 Maribor, Slovenia
Tel.: +386-31-659-279, +386-2-220-7662
E-mail: nenad.gubeljak@uni-mb.si

Doc. dr. Jožef Predan
University of Maribor
Faculty of Mechanical Engineering
Smetanova ul. 17, 2000 Maribor, Slovenia
Tel.: +386-31-659-279, +386-2-220-7662
E-mail: jozef.predan@uni-mb.si